16TH EUROPEAN CONFERENCE ON EARTHQUAKE ENGINEERING THESSALONIKI 18 - 21 JUNE 2018

ACCURATE ESTIMATION OF STRONG GROUND MOTIONS AND SIMULATION OF STRUCTURAL DAMAGE AT KUMAMOTO PORT DURING THE 2016 KUMAMOTO EARTHQUAKE

Masayuki YAMADA[1], Akito SONE[2], Naonori KUWABARA[2], Kenji EBISU[2], Shuji YAMAMOTO[3], Masahiro SATO[4], Takashi KIDOU[5]

ABSTRACT

In Japan, port facilities are designed and constructed according to the "Technical Standards and Commentaries for Port and Harbor Facilities in Japan" (hereinafter called the "Technical Standards"). The 2016 Kumamoto Earthquake caused, if not considerable, damage to structures at Kumamoto Port, including cracks on quay walls, settlement of crane foundation and deformation of movable bridges. To validate the analyses in the Technical Standards, the authors first estimated strong ground motions at Kumamoto Port. Secondly, the authors conducted two-dimensional effective analyses for two afflicted quay walls with the water depth of -7.5m and -5.0m, with the ground motions estimated. The analyses more or less reproduced the displacement volumes and the state of damage to the quay walls, so the authors confirmed the validity of the Technical Standards and designing based on the Standards.

Keywords: the 2016 Kumamoto Earthquake, the corrected empirical Green's function method, the two-dimensional effective stress analysis, Kumamoto port, damage reproducing

1. INTRODUCTION

A magnitude M_j 6.5 (M_w6.2) earthquake and a magnitude M_j 7.3 (M_w7.0) earthquake occurred in Kumamoto Prefecture, Japan at 21:26 JST on April 14, 2016, and 01:25 JST on April 16, respectively. The 2016 Kumamoto Earthquake including these (hereinafter called the "Kumamoto-eq.") were recorded the Japanese seismic coefficients of 7 in Mashiki town and Nishihara village in Kumamoto Prefecture, and the seismic coefficients of 6-lower to 6-upper in the Kumamoto City and Aso District. They caused severe damage to wide areas with numerous ground disasters including slope failure causing the collapse of Aso-ohashi Bridge (Kasama et al. 2017).

In Japan, port facilities are designed and constructed according to the Technical Standards. In the latest version of the Technical Standards, two-dimensional effective stress analyses are widely used. However, the accuracy of the analyses should be subject to further validation in terms of the applicability to improved soils and special structures. The Kumamoto-eq. provided rare opportunities for the validation. Damage to structures at Kumamoto Port includes horizontal displacement of a

[1]NEWJEC Inc. Earthquake engineering team, Technology Development group, 3-20 Honjo-Higashi 2-chome, Kita-ku, Osaka, Japan, yamadams@newjec.co.jp

[2]NEWJEC Inc. Coastal disaster prevention team, Port and coastal engineering group, 3-20 Honjo-Higashi 2-chome, Kita-ku, Osaka, Japan, sonekt@newjec.co.jp, kuwabarann@newjec.co.jp, ebisukn@newjec.co.jp

[3]Coastal Development Institute of Technology, Shimbashi SY Bldg.5F, 1-14nishishinbashi 2-chome, minatoku, Tokyo, Japan, s_yamamoto@cdit.or.jp

[4]Coastal Development Institute of Technology, Shimbashi SY Bldg.5F, 1-14nishishinbashi 2-chome, minatoku, Tokyo, Japan, m_satou@cdit.or.jp

[5]The Shimonoseki Research and Engineering Office for Port and Airport, Kyushu Regional Development Bureau, Ministry of Land, Infrastructure and Transport, 6-4 Takezakisho 4-chome, Shimonoseki, Yamaguchi, Japan, kidou_t8910@mlit.go.jp

caisson quay wall, settlement of crane foundation and deformation of movable bridges, but was not great. The damage to the quay wall was only slight probably as it stood on soil improved by the sand compaction pile (SCP) method.

To validate the analyses in the Technical Standards, the authors estimated strong ground motions at Kumamoto Port and conducted two-dimensional effective stress analyses to reproduce structural damage at Kumamoto Port.

2. ACCURATE ESTIMATION OF STRONG GROUND MOTIONS AT KUMAMOTO PORT DURING THE KUMAMOTO-EQ.

No seismograph existed at Kumamoto Port, so that no record of ground motions was obtained during the magnitude M_j 6.5 earthquake at 21:26 JST on April 14, 2016 (hereinafter called the "foreshock") and the magnitude M_j 7.3 earthquake at 01:25 JST on April 16 (hereinafter called the "main shock") in the Kumamoto-eq. Therefore, the authors observed aftershocks right after the main shock, and calculated, with the observation data, the main shock ground motions by the corrected empirical Green's function method (hereinafter called the "C-EGF method") and the site effect substitution method (hereinafter called the "SES method").

Estimation of ground motions by the C-EGF and SES methods requires the site amplification factor(seismic bedrock to engineering bedrock) of Kumamoto Port, for which the authors referred to a factor available to the public (http://www.ysk.nilim.go.jp/kakubu/kouwan/sisetu/) shown in Figure 1. The factor is predominant in low-frequency band, having a peak around 0.2 to 0.3Hz.

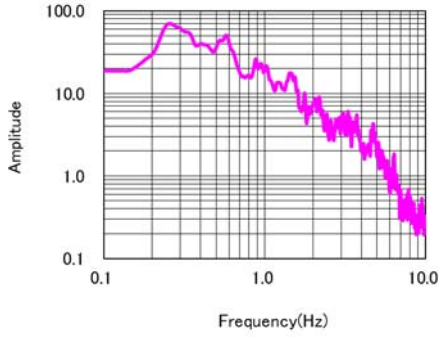

Figure 1. Site Amplification Factor of Kumamoto Port (Seismic Bedrock to Engineering Bedrock)

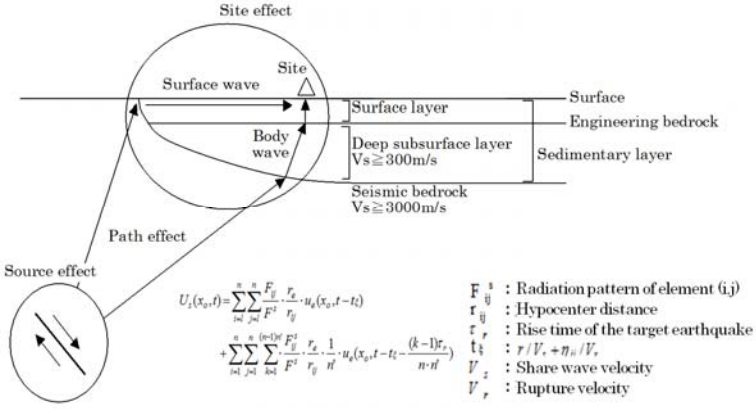

Figure 2. Conceptual Diagram of the C-EGF Method

2.1 Estimation of strong ground motions by the corrected empirical Green's function method

2.1.1 The characterized source models and the corrected empirical Green's function method

The ground motions were calculated by the C-EGF method considering soil nonlinearity with the characterized source model by Nozu (Nozu et al. 2016a, Nozu et al. 2016b), which can reproduce strong ground motions at 10 observation stations near the source region including K-NET, KiK-net and other stations. The same source model was applied to simulating strong ground motions at the Shirakawa (Oshima) observatory, the strong motion station closest to Kumamoto Port. The result was fairly consistent with the observed records in terms of velocity waveforms and Fourier spectra, indicating the applicability of the nonlinear parameters for the simulation. Finally, the same source model and the same nonlinear parameters were used to simulate strong ground motions at Kumamoto Port. Figure 2 illustrates a conceptual diagram of the C-EGF method, and Figure 3 shows the characterized source model.

Asperity		1	2	3
Hypocenter	Longitude(deg)	130.802	130.823	130.898
	Latitude(deg)	32.783	32.797	32.841
	Depth(km)	15.0	15.0	11.0
Length(km)		1.5	3.0	4.0
Width(km)		1.5	3.0	5.0
Seismic moment(Nm)		1.00E+24	2.50E+24	2.50E+25
Rupture start time(s)		0.0	0.9	4.1
Rupture velocity(km/s)		2.8	2.8	2.8
Rise time(s)		0.13	0.27	1.00
Number of partitions		5×5×5	5×5×5	10×10×10

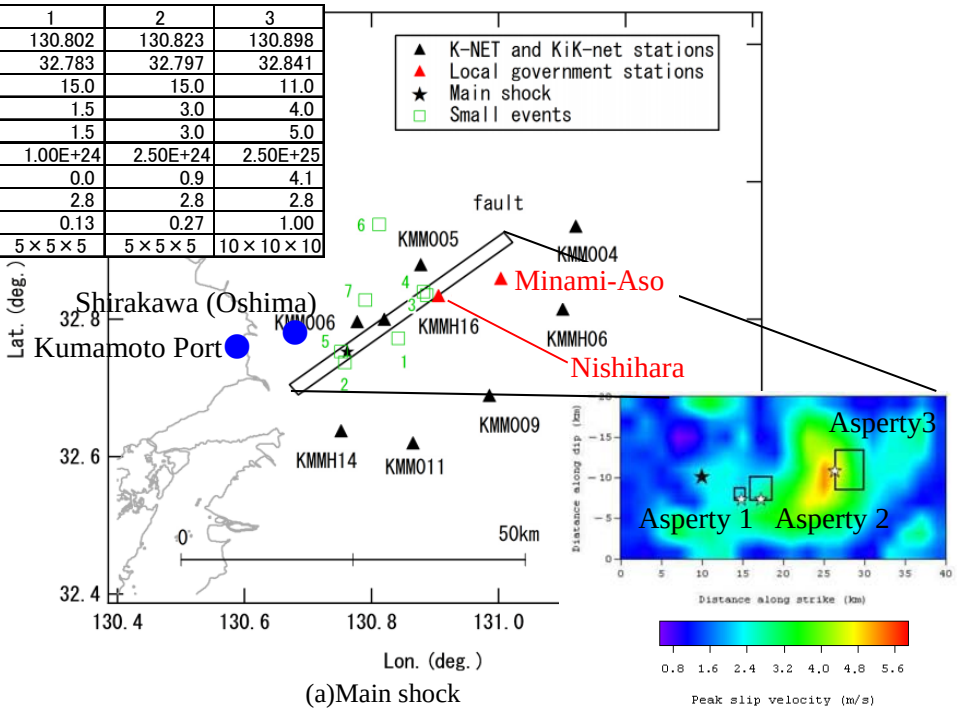

(a)Main shock

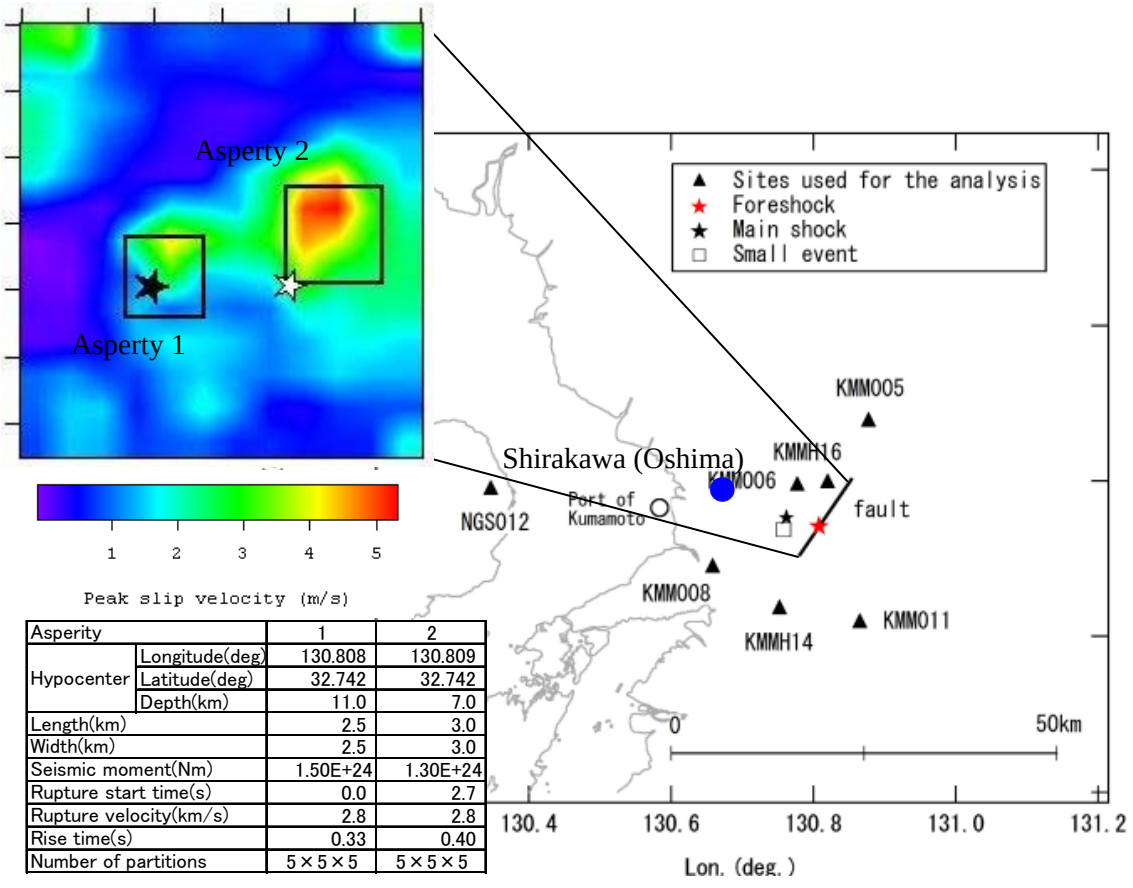

Asperity		1	2
Hypocenter	Longitude(deg)	130.808	130.809
	Latitude(deg)	32.742	32.742
	Depth(km)	11.0	7.0
Length(km)		2.5	3.0
Width(km)		2.5	3.0
Seismic moment(Nm)		1.50E+24	1.30E+24
Rupture start time(s)		0.0	2.7
Rupture velocity(km/s)		2.8	2.8
Rise time(s)		0.33	0.40
Number of partitions		5×5×5	5×5×5

(b)Foreshock

Figure 3. Characterized Source Model

Table 1. Nonlinear and other parameters

	Nonlinear parameters		PRTITN	
	ν 1	ν 2	N25.2° E	N115.2° E
Main shock	0.86	0.10	0.53	0.85
Foreshock	0.95	0.01	0.53	0.85

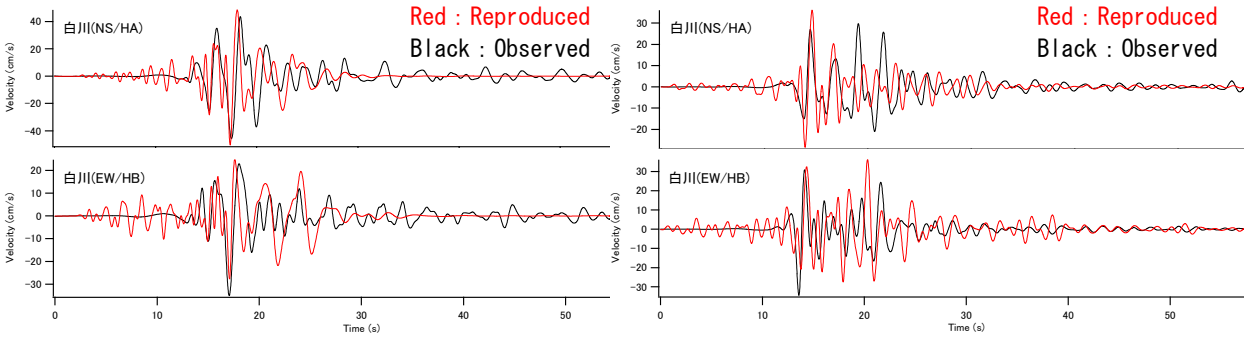

(a)Main shock (b)Foreshock

Figure 4. Reproduced and Observed Velocity Waveforms at Shirakawa (Oshima)Observatory

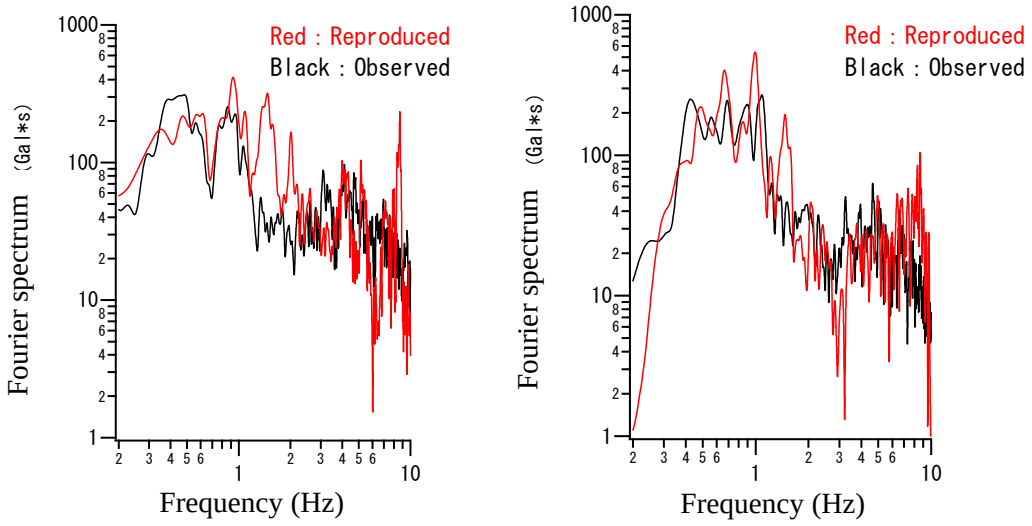

(a)Main shock (b)Foreshock

Figure 5. Reproduced Fourier Spectra at Shirakawa (Oshima) Observatory

2.1.2 Reproduction of observation records at the Shirakawa (Oshima) observatory and estimation of strong ground motions at Kumamoto Port

The same source model was applied to simulating strong ground motions at the Shirakawa (Oshima) observatory, the station closest to Kumamoto Port. The result was fairly consistent with the observed records in terms of velocity waveforms and Fourier spectra, indicating the applicability of the nonlinear parameters for the simulation. Table 1 lists the nonlinear and other parameters used, and Figures 4 and 5 show the velocity waveforms and Fourier spectra reproduced at the Shirakawa (Oshima) observatory.

Finally, the same source model and the same nonlinear parameters were used to simulate strong ground motions at Kumamoto Port. Figure 6 shows the results of the estimation.

2.2 Estimation of strong ground motions by the site effect substitution method

The SES method (for example, Hata et al. 2012) is assumed that the phase factor of a large earthquake is considerably affected by the site effect. The SES method is a method of estimating strong motions

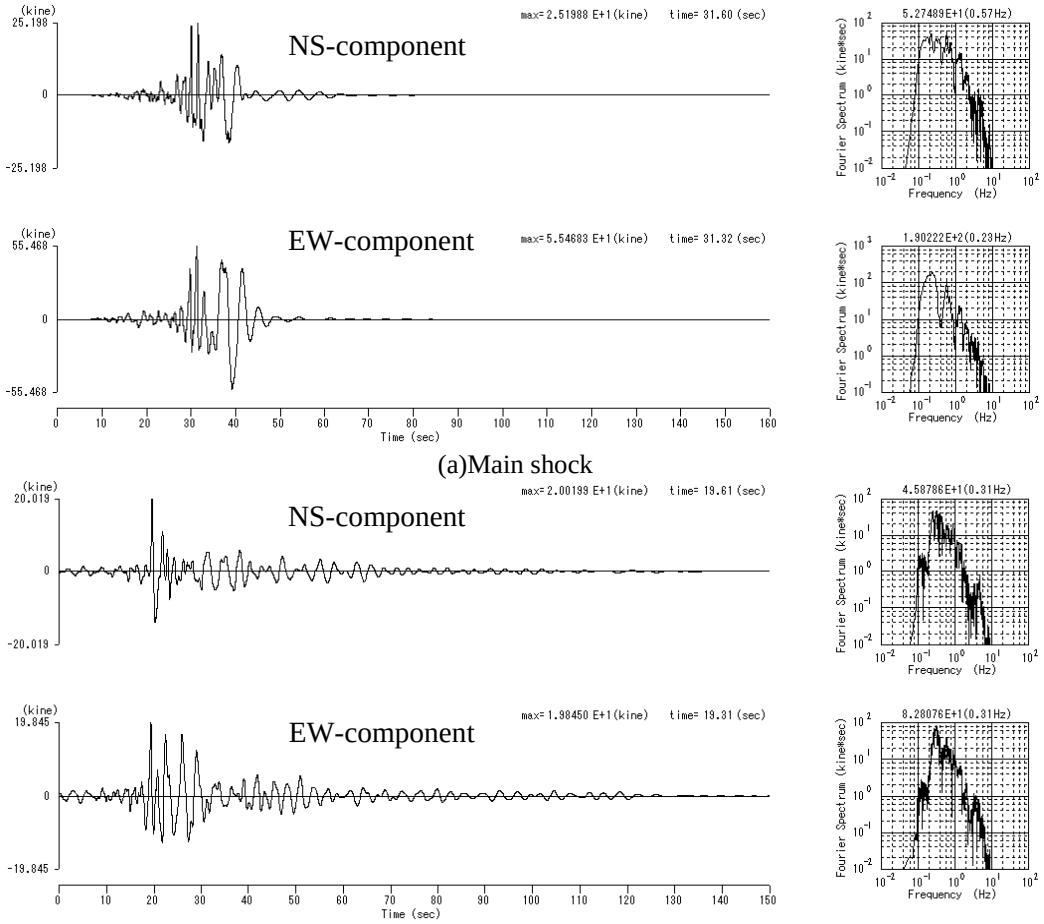

(a)Main shock

(b)Foreshock

Figure 6. Estimation of Strong Ground Motions at Kumamoto Port
(left: Velocity waveforms, right: Fourier spectra)

of large earthquakes that the site amplification and phase factors of the nearby observatory is removed from the strong motion of large earthquake of nearby observatory and that the site amplification factor and the phase factor of the aftershock record of the objective site is substituted in question for them. The authors estimated seismic ground motions at Kumamoto Port for the Kumamoto-eq. by the SES method with the main shock and foreshock records at the Shirakawa (Oshima) observatory as the nearby site. However, the calculated motions were larger than those estimated by the C-EGF method, probably because it was difficult to take into account the effect of soil nonlinearity in this scheme.

Figure 7 shows the results of estimation of strong ground motions by the SES method. The aftershocks at Kumamoto Port used as the phase factors corresponded with the aftershocks at the Shirawaka (Oshima) observatory that the calculated motions which were substituted the phase factors of aftershocks for the phase factors of the main shock and foreshock were the most consistent with the observed motions of the main shock and foreshock at the Shirawaka.

2.3 Evaluation of calculated strong ground motions by the two methods

Figure 8 shows comparison of acceleration response spectra of strong ground motions estimated by the two methods. For the estimated strong ground motions of both the main shock and foreshock, the results of the C-EGF method and the SES method generally corresponded in longer period than 0.5 seconds. In shorter period than 0.5 seconds, on the other hand, the estimation by the SES method was found to be larger. This was consistent with the fact that the peak ground velocity, PGV, was greater in terms of velocity waveforms. We decided that the strong ground motions estimated by the C-EGF method were more accurate than by the SES method, because the results of strong ground motions reproduced at the Shirakawa (Oshima) observatory were fairly consistent.

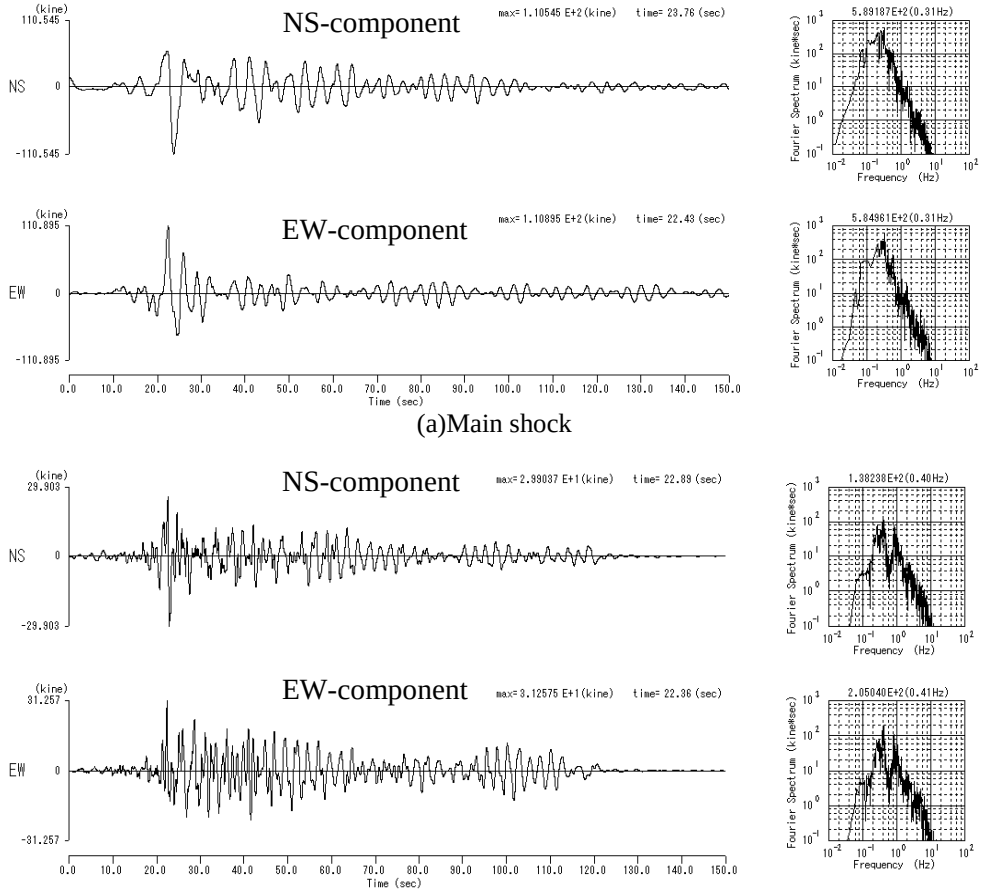

(a)Main shock

(b)Foreshock

Figure 7. Estimation of Strong Ground Motions by the SES Method
(left: Velocity waveforms, right: Fourier spectra)

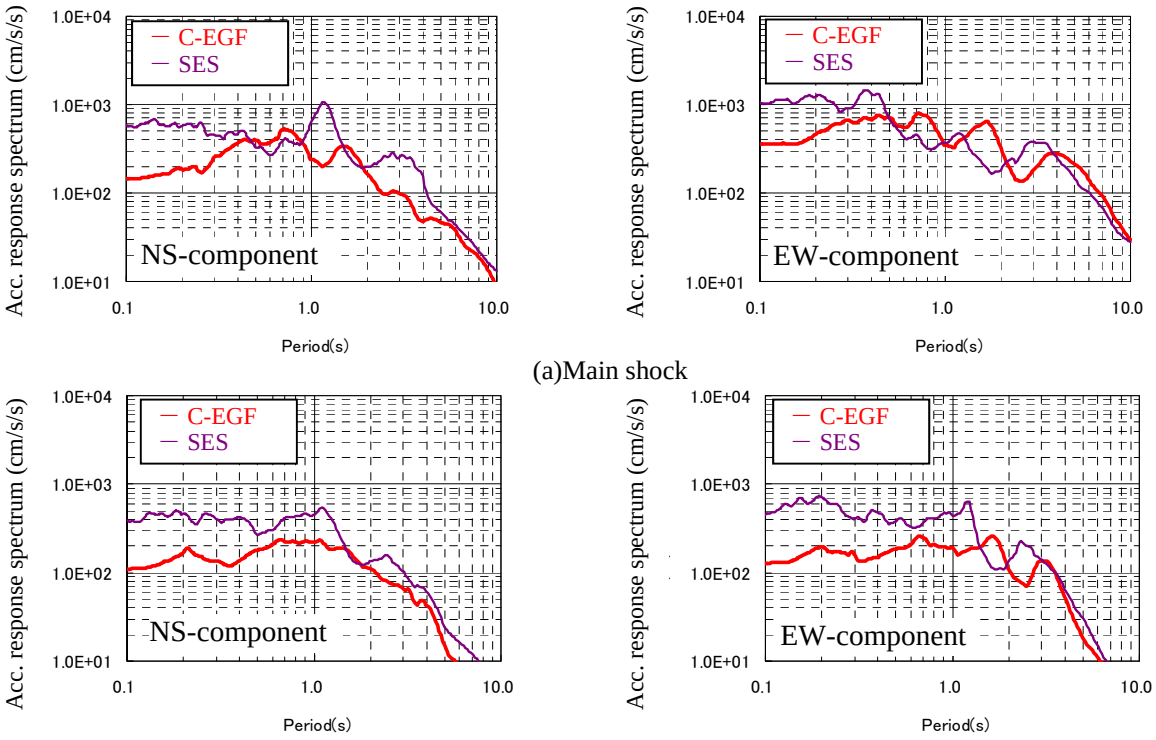

(a)Main shock

(b)Foreshock

Figure 8. Comparison of Strong Ground Motions Estimated by the Two Methods
(Acceleration response spectrum, h=5%)

To evaluate the extent of the estimated ground motions affecting the port facilities qualitatively, the motions were compared with the level-one (L1) and level-two (L2) design ground motions in terms of acceleration response spectrum. The estimated motion for the main shock was larger than the L1 design ground motion, but smaller than the L2 design ground motions at Kumamoto Port in terms of acceleration response spectrum. The estimated motion for the foreshock was close to the L1 design ground motion in both of NS and EW components (Figure 9).

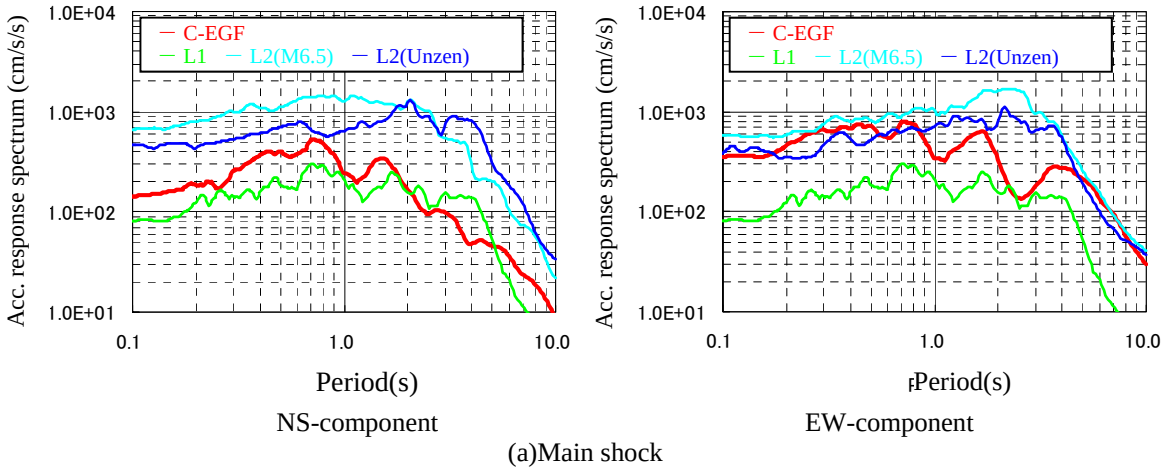

NS-component EW-component

(a)Main shock

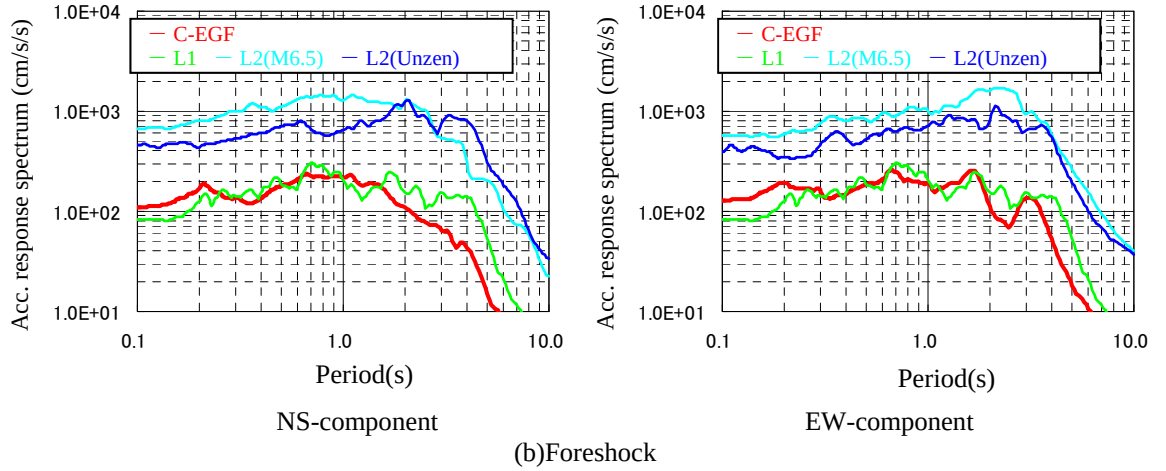

NS-component EW-component

(b)Foreshock

Figure 9. Comparison of Estimated and Design Strong Ground Motions
(Acceleration response spectrum, h=5%)

3. SIMULATION OF STRUCTURAL DAMAGE DURING THE KUMAMOTO-EQ.

3.1 Port facilities to be examined, and their structural damage by the Kumamoto-eq.

Figure 10 shows the location of the port facilities we examined, and Table 2 provides a summary of the facilities, covering their structural type, design year, design standards, and design seismic coefficients. Figures 11 and 12 show typical cross-sections of the quay walls (-7.5m and -5.0m) of Kumamoto Port, respectively. Structurally, the former is a gravity caisson quay wall, and the latter is a movable bridge on a pile foundation. As for the design standards, the former is designed by the safety factor method in compliance with the 1979 edition of the Technical Standards, and the latter by the seismic coefficients method in compliance with the 1989 edition. As for the ground property at Kumamoto Port, soft Ariake clay deposits exist deep down to DL-40m.

Damages to the -7.5m quay wall by the earthquakes included cracks and vertical displacement near the

crane foundation, and buckling deformation of the quay wall itself. According to control point surveys conducted before and after the earthquakes, October 2013 and June 2016 respectively, the relative displacements were approximately 12cm to the south (perpendicular to the normal line of the wall, to the seaside) and approximately 3cm to the west (parallel to the normal line) (The Shimonoseki Research and Engineering Office, 2016). Another vertical displacement of approximately 7cm was observed at the crane foundation on the land side[8]. Moreover, the ground liquefaction distant from the quay wall caused subsidence of the pavement and other damage, but the area immediately behind the quay wall was not liquefied, and the displacement of the quay way was relatively minor. Nozu et al. 2017 attribute this minor damage mostly to soil improvement carried out by the SCP method (improvement rate of 80%), which was conducted to reinforce the entire alluvial formation beneath the caisson quay wall. The liquefaction countermeasure by the SCP method appears to be effective in the area immediately behind the quay wall (improvement rate of 15%). As for the -5.0m quay wall, a side roller at the gatepost was displaced by 6cm, causing problem with the movable bridge for vehicles boarding ferries (The Shimonoseki Research and Engineering Office, 2016).

3.2 Static analysis and study (comparison of action and limit seismic intensities)

To validate the design concept of the -7.5m quay wall, the authors compared the active and critical seismic intensities calculated according to the seismic coefficients equation for verification in the Technical Standards 2007 edition. The equation is given below (The Ports and harbours Association of Japan, 2007). If the active seismic coefficients are smaller than the critical seismic coefficients, the quay wall is predicted to be undamaged. If the active seismic coefficients are greater than the critical seismic coefficients, the quay wall is predicted to be damaged. Then, the authors checked the displacement calculated against the presence of displacement actually observed on the site. Here, the authors defined that the term “active seismic coefficients” means the seismic coefficients calculated with the simulation formula on the basis of the strong ground motions simulated in this study for the Kumamoto-eq. (or the strong ground motions actually observed); and that the term “critical seismic coefficients” means the seismic coefficients for the gravity quay wall concerned when the safety factor of any of the three failure modes -- sliding, overturning, and bearing capacity -- equals 1.0

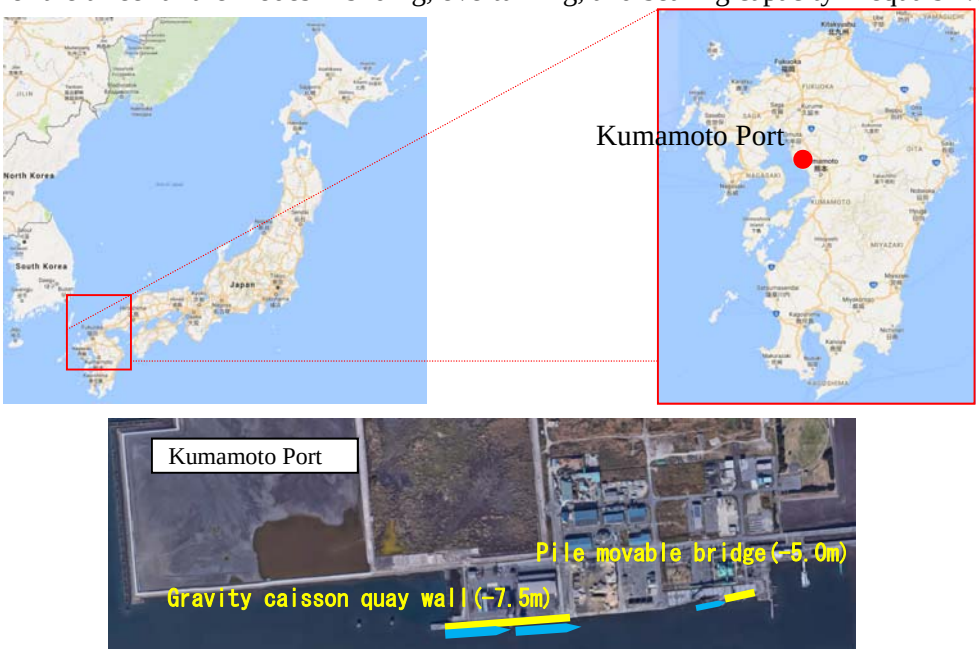

Figure 10. Location of the Port Facilities

Table 2. Summary of the Port Facilities

Port	district	facility	structual type	design year	design standards	design seismic intensity
Kumamoto Port	Yumesakishima	quay wall(−7.5m)	gravity caisson	1988	Technical Standards (1979)	0.16
		quay wall(−5.0m)	movable bridge	1989	Technical Standards (1989)	0.1

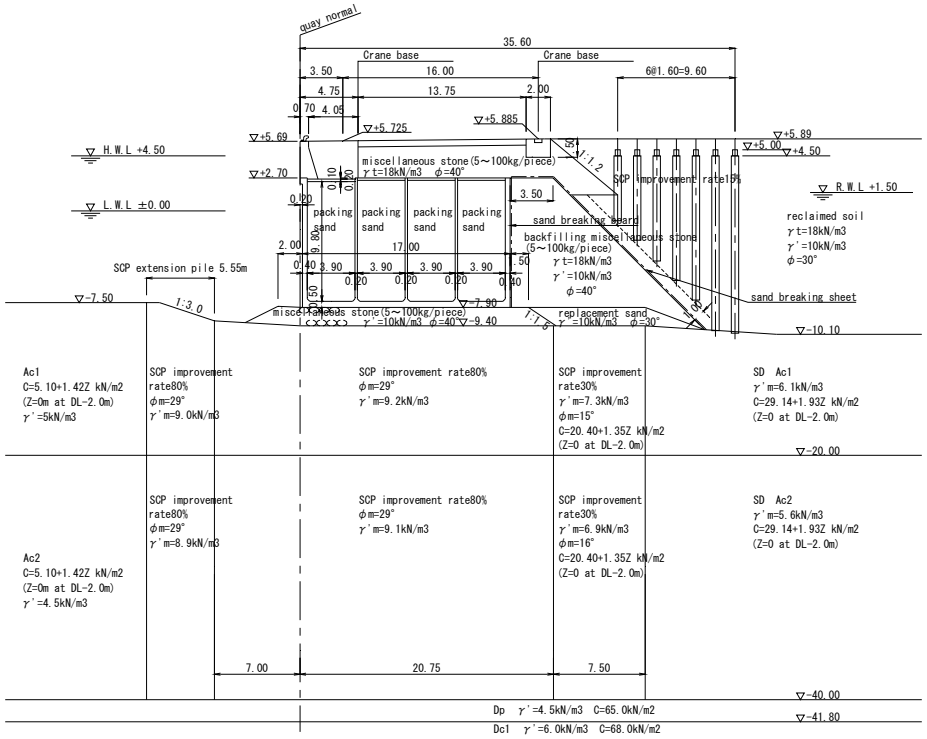

Figure 11. The -7.5m Quay Wall of Kumamoto Port (Yumesaki Island), Gravity Quay Wall

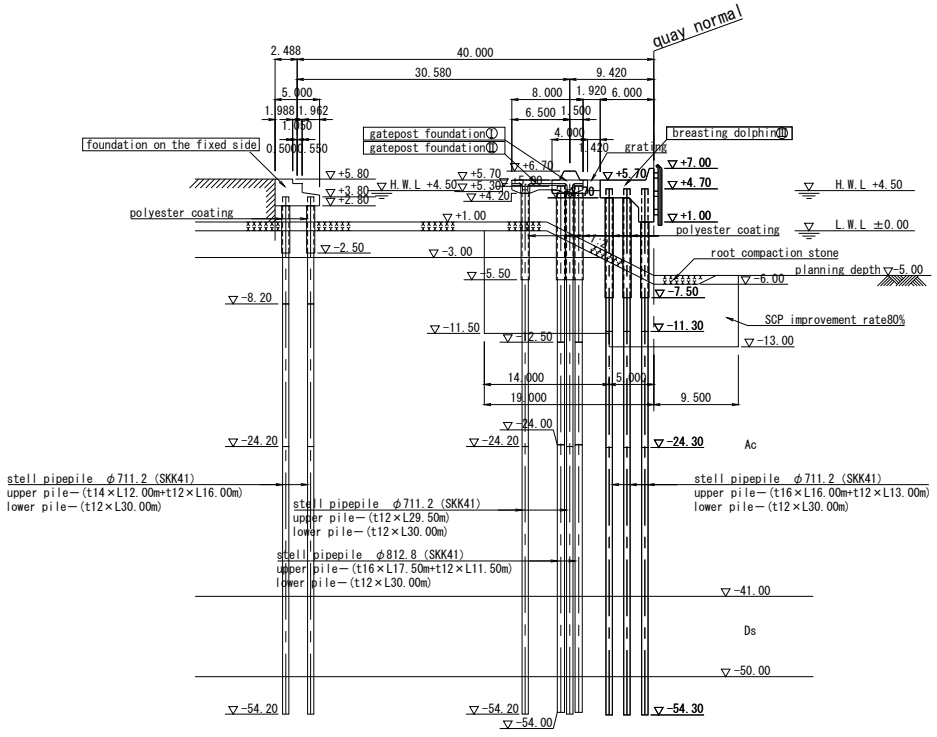

Figure 12. The -5.0m Quay Wall of Kumamoto Port (Yumesaki Island), Movable Bridge

$$k_{h_k} = 1.78\left(\frac{D_a}{D_r}\right)^{-0.55}\frac{\alpha_c C}{g} + 0.04 \quad (1),$$

where

K_h : characteristic value of the seismic coefficients against the Level one Earthquake Ground Motion

D_a : allowable displacement at the crown of the mooring wharf (=10cm),

D_r : standard displacement (=10cm),

α_c : maximum correction acceleration (cm/s^2),

C : reduction coefficient of seismic charactristics due to improved subsoil (C=0.75), and

g : gravitational acceleration (=980cm/s^2).

The active seismic coefficients (0.14) were smaller than the critical seismic coefficients (0.20) for the -7.5m quay wall. It was predicted to be unscathed but actually suffered from displacement of over 10cm (greater than Da=10cm). (The quay wall was officially judged "damaged".) The determinant of the critical seismic coefficients were displacement among three failure modes.

Figure 13 shows a criterion chart using allowable displacement, proposed by Fukunaga et al. *Da*=10cm denotes the standard value of *Da* for gravity quay walls. There are cases of 41 gravity quay walls with the water depth from -7.5m to -14.6m plotted in the chart, and the authors added a red triangle presenting the results of this study. The vertical axis shows the critical seismic coefficients and the horizontal axis the active seismic coefficients. If the active seismic coefficients are greater than the critical seismic coefficients, the quay wall in question is plotted in the lower right domain (in grey) and predicted to be damaged. If the active seismic coefficients are equal to or smaller than the critical seismic coefficients, the quay wall in question is plotted in the upper left domain (in white) and predicted to be undamaged.

The black triangles indicate the quay walls actually damaged, and the inverted white triangles the quay walls actually undamaged. The chart enables us to visually check if a simulation result matches the actual state of damage, and whether a simulation result gives a sign of danger or safety. If a prediction made according to a design simulation and a judgment about the actual state are in agreement that the structure in question is to be “damaged” or “undamaged”, in other words, if the simulation predicts the reality correctly, the judgment about damage to the structure in question is correct. In this case, the evaluation is deemed “matched”. Suppose that a design simulation predicts that the structure in question will not be damaged as the active seismic coefficients are smaller than the critical seismic coefficients, but that the structure was damaged in reality. Then, the active seismic coefficients were likely to be underestimated, so the evaluation is deemed “danger”. On the other hand, if a simulation concludes that the structure will be damaged but it remained undamaged in reality, the active seismic coefficients were likely to be overestimated. In this case, the evaluation is deemed “safe” (Fukunaga et al. 2016).

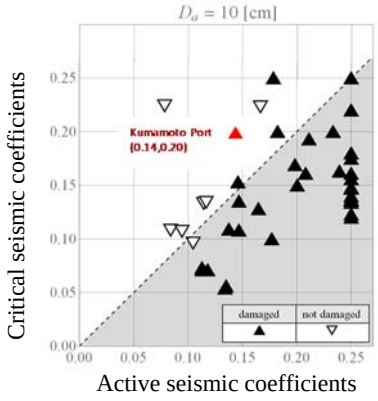

Figure 13. Comparison of Active and Critical Seismic Intensities [added to Fukunaga et al. 2016],
Gravity Quay Walls with water depth from -7.5m to -14.6m
(Comparison of the Results of Verification of Damage in This Study and Other Facilities)

For the -7.5m gravity quay wall of Kumamoto Port, the simulation result failed to match the reality, and the evaluation was thus deemed “danger”. The proportion of evaluations made for other facilities and deemed “danger” was 7.3% (three facilities), and the proportion of evaluations deemed “matched” was 90.2% (37 facilities).

3.3 The effective stress analysis and study (Calculation of displacement volume, etc.)

This section examines the impact of estimated strong ground motions on displacement of quay walls by performing seismic response analysis on the facilities, and comparing the displacement obtained with the analysis with the actual damage to them. For the seismic response analysis, the authors used the effective stress analysis code FLIP, which takes into account a nonlinear model of the soil (Iai et al.

1992a and Iai et al. 1992b).

Table 3 shows the displacement simulated by the effective stress analysis focusing on displacement of the upper and lower ends of the quay walls, and of each pile in the foundation of the movable bridge. The relative displacement was approximately 0.10m to the seaside between the upper and lower ends. The displacement of the foundation underneath the caisson quay wall accounted for approximately 65% of all the horizontal displacement. The inclination angle was approximately 0.45 degrees. The simulation results were roughly close to the actual displacement of the gravity quay wall, which was approximately 0.13m to the seaside. Figure 14 shows simulated displacement highlighting the caisson quay wall.

As for the -5.0m quay wall, the authors simulated and obtained the horizontal displacement shown in Table 3. The relative displacement of gatepost foundations A and B indicates that the displacement of gatepost foundation A is greater, if not considerably. Examinations on steel materials show that none of the piles suffer from the full plastic. In reality, the quay wall was moved in longitudinal direction to the offshore. The foundation on the fixed side was moved by 0.03m (to the offshore), and gatepost foundation A was moved more than gatepost foundation B. The simulation results were roughly similar to the actual damage.

Table 3. Displacement Volumes Simulated by The effective stress

facility	method	position	horizontal displacement (m)	vertical displacement (m)
quay wall(−7.5m)	C-EGF method	quay upper	0.28	0.11
		quay lower	0.19	0.11
quay wall(−5.0m)		breasting dolphin	0.08	0.00
		gatepost foundationA	0.08	0.00
		gatepost foundationB	0.07	0.00
		foundation on the fixed side	0.04	0.00

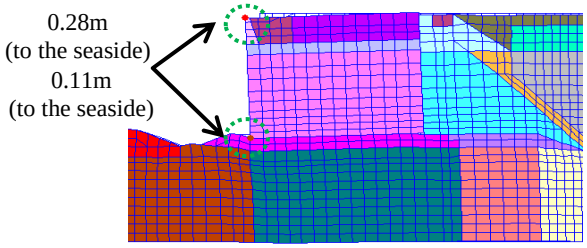

Figure 14. Part of Displacement Diagram of the -7.5m Quay Wall at Kumamoto Port

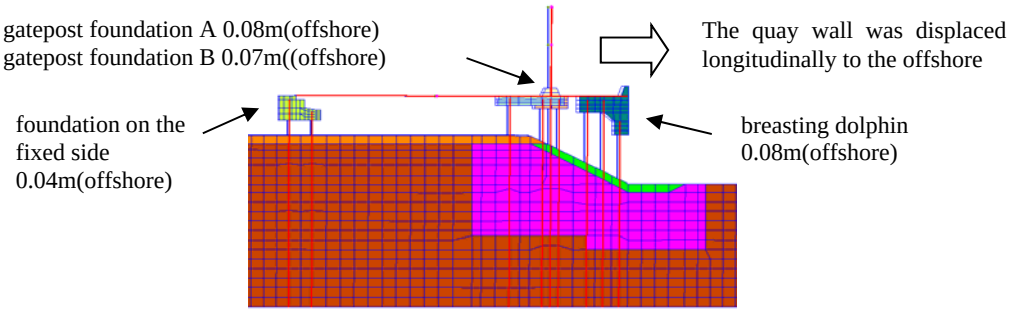

Figure 15. Part of Displacement Diagram of the -5.0m Quay Wall at Kumamoto Port

4. CONCLUSIONS

This study examined the impact of the 2016 Kumamoto Earthquake on port facilities, the -7.5m and -5.0m quay walls at Kumamoto Port. The findings are summarizes as follows. The authors hope that the study will contribute to future planning of quay walls. (i) The authors first estimated strong ground

motions at Kumamoto Port by the C-EGF method. Comparison was made between the estimated ground motions, and the L1 and L2 design ground motions. The estimated ground motions of the foreshock were smaller than or close to those of the L1 design ground motions. The value for the ground motions estimated for the main shock fell in between the L1 and L2 design ground motions. This indicates that strong ground motions affected the port facilities. (ii) Static analysis was conducted to compare the active and critical seismic coefficients . The simulation result failed to match the reality of the -7.5m quay wall at Kumamoto Port, and thus the evaluation was deemed “danger”, if not considerably. (iii) The effective stress analysis was conducted to calculate the displacement volume. The calculated volumes were found to be more or less close to the actual state of damage to the -7.5m and -5.0m quay walls at Kumamoto Port.

5. ACKNOWLEDGMENTS

We are grateful to Dr. Nozu for helpful discussions and permission to use the characterized source models for the 2016 Kumamoto Earthquake. We thank for permission to use the seismic records of K-NET and KiK-net by National Research Institute for Earth Science and Disaster Resilience and the seismic records at the Shirakawa (Oshima) observatory by Ministry of Land, Infrastructure, Transport and Tourism in Japan.

6. REFERENCES

Kasama, K., Kitazono, Y., Yakabe, H. (2017). Reconnaissance Report on Slope Disaster Caused by the 2016 Kumamoto Earthquake, the Geotechnical Engineering Magazine, No. 711, pp8-11.

National Institute for Land and Infrastructure Management, Port and Harbor Department, Port Facilities Division, the Ministry of Land, Infrastructure, Transport and Tourism, http://www.ysk.nilim.go.jp/kakubu/kouwan/sisetu/

Nozu, A. (2016)a. Characterized Source Models for the M7.3 Main Shock of the 2016 Kumamoto Earthquake, http://www.pari.go.jp/bsh/jbn-kzo/jbn-bsi/taisin/sourcemodel/somodel_2016kumamoto.html

Nozu, A. (2016)b. Characterized Source Models for the M6.5 Foreshock of the 2016 Kumamoto Earthquake, 2016, the website of the Port and Airport Research Institute, http://www.pari.go.jp/bsh/jbn-kzo/jbn-bsi/taisin/sourcemodel/somodel_2016kumamoto_z.html

Nozu, A. and Morikawa H. (2003) An Empirical Green’s Function Method Considering Multiple Nonlinear Effects, the Journal of the Seismological Society of Japan. 2nd ser., Vol. 55, No. 4, pp. 361-374.

Hata, Y., Ichii, K., Tokida, K., Nozu, A., Yokota, S., and Kaneta, K. (2012). Strong Motion Estimation at the Embankment of the Joban Expressway Damaged by the 2001 Off the Pacific Coast of Tohoku Earthquake and Its largest Aftershock Based on Site Effect Substitution Method, the Journal of the Japan Society of Civil Engineers, A1: Structural Engineering/Earthquake Engineering, Vol. 68, No. 4, pp I_315-330.

The Shimonoseki Research and Engineering Office for Port and Airport, Kyushu Regional Development Bureau, Ministry of Land, Infrastructure and Transport (2016). FY2015 Technical Issues to Be Considered.

Nozu, A. and Kohama, E. (2017). Damage to Port Structures during the 2016 Kumamoto Earthquake Sequence, the Geotechnical Engineering Magazine, No.711, pp36-39.

The Ports and harbours Association of Japan (2007). The Technical Standards and Commentaries for Port and Harbor Facilities in Japan, Vol. 2, pp955, pp994.

Fukunaga, Y., Takenobu, M., Miyata, M., Nozu, A., Kohama, E. (2016). Evaluation of Validity of the Seismic Coefficients Equation for Verification by Inspection of Damage to Gravity and Sheet-Pile Quay Walls, National Institute for Land and Infrastructure Management, No.920.

Iai, S., Matsunaga, Y. and Kameoka, T. (1992)a. Strain space plasticity model for cyclicmobility, Soils and Foundations, Vol. 32, No.2, pp.1-15.

Iai, S., Matsunaga, Y. and Kameoka, T. (1992)b. Analysis of undrained cyclic behavior of sand under anisotropic consolidation, Soils and Foundation , Vol. 32, No.2, pp.16-20.